Geophysical Research Letters

Supporting Information for

Warm phase of AMV damps ENSO through weakened thermocline feedback

Paloma Trascasa-Castro[1], Yohan Ruprich-Robert[2], Frederic Castruccio[3], Amanda C. Maycock[1]

[1] School of Earth and Environment, University of Leeds, Leeds, UK

[2] Barcelona Supercomputing Center, Barcelona, Spain

[3] National Center for Atmospheric Research, Boulder, CO, USA

Contents of this file

- Figures S1 to S5
- Detailed methodology

Introduction

This document provides additional graphic information to support our results, including the sea surface temperature (SST) anomaly pattern associated with the positive phase of the Atlantic Multidecadal Variability (AMV) and El Niño Southern Oscillation (ENSO), a decomposition of the AMV modulation of ENSO feedbacks in its individual terms and an illustration of the linearity of the SW and β_h terms.

Additionally, this document contains detailed instructions to calculate the Bjerknes Stability index.

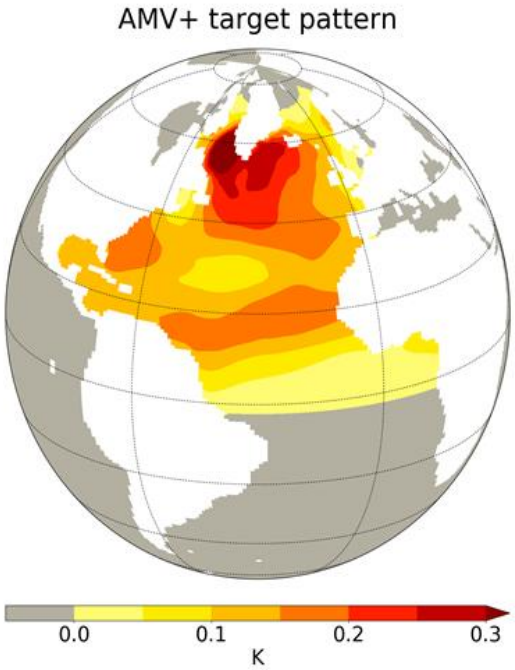

Figure S1. Target AMV+ sea surface temperature (SST) pattern. The AMV- is equivalent in amplitude but with opposite sign SST anomalies.

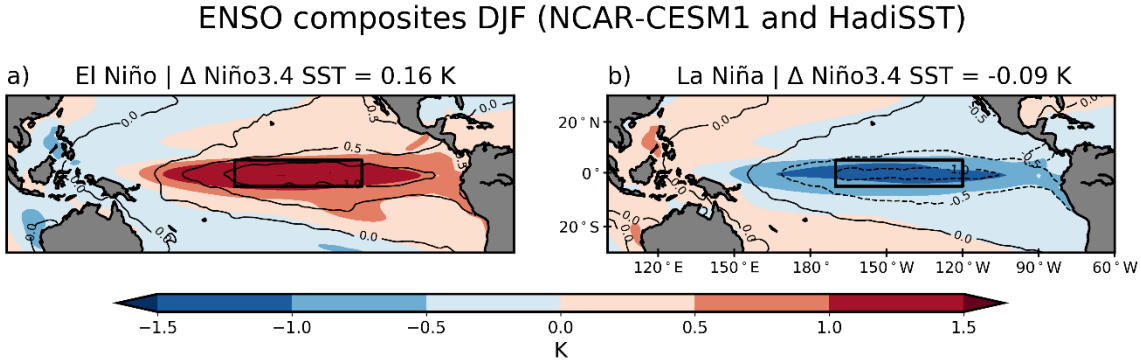

Figure S2. El Niño (a) and La Niña (b) SST anomaly composite in NCAR-CESM1 (filled contours) and observations (HadiSST, black contours). The differences in Niño3.4 SST anomalies between the model and observations is 0.16 K for El Niño and -0.09 for La Niña. The black rectangle denotes the Niño3.4 region (5°N-5°S, 170°E-120°E)

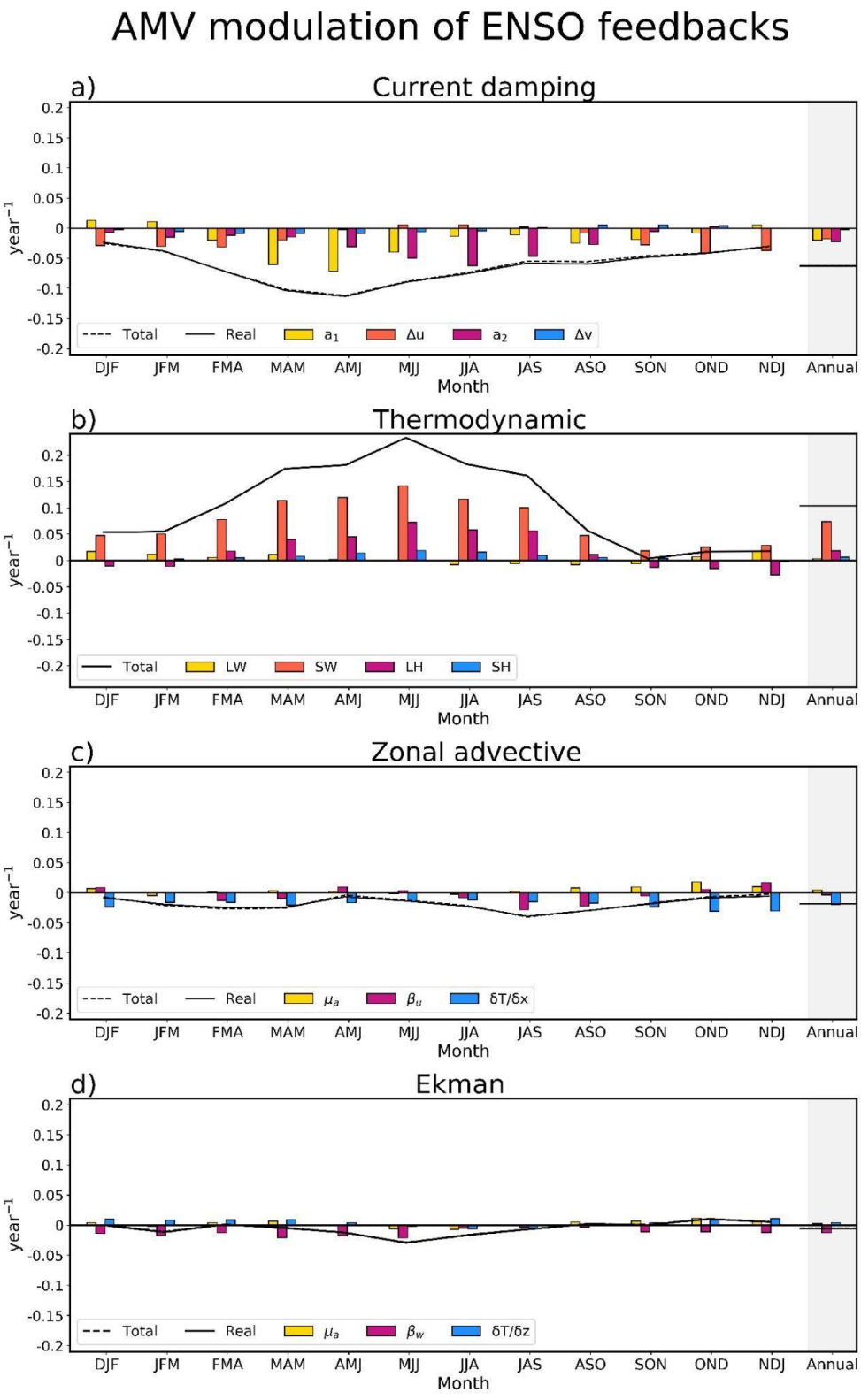

Figure S3. AMV modulation of the a) current damping, b) thermodynamic, c) zonal advective and d) Ekman feedbacks, decomposed onto their independent terms to homogenize their units. Monthly values are smoothed with a 3-month running mean.

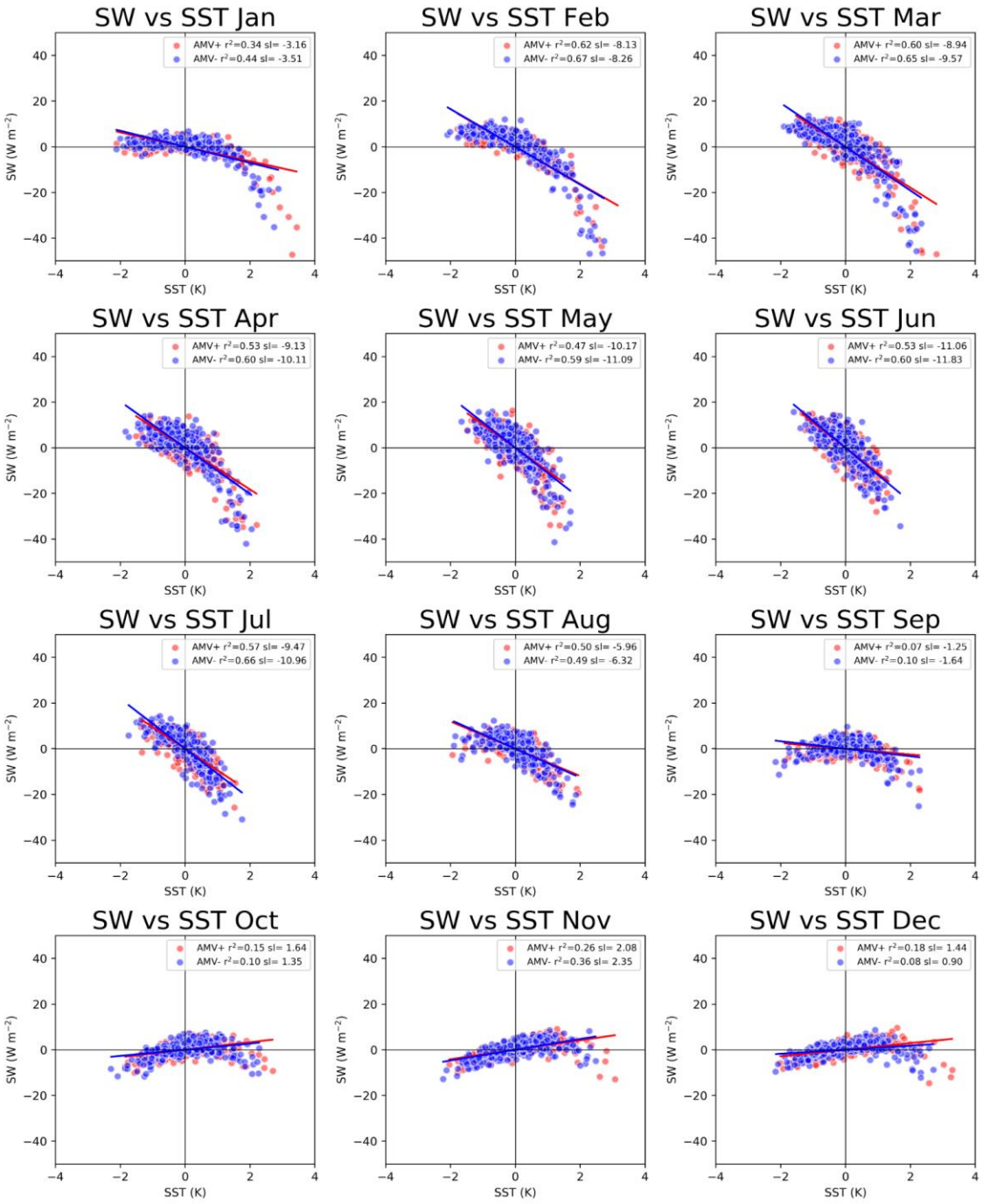

Figure S4. Scatterplot of monthly east Pacific shortwave radiation anomalies vs. east Pacific sea surface temperature anomalies in the AMV+ (red) and AMV- (blue) experiments. The legend shows the regression slope (W m^{-2} K^{-1}) and r^2 value.

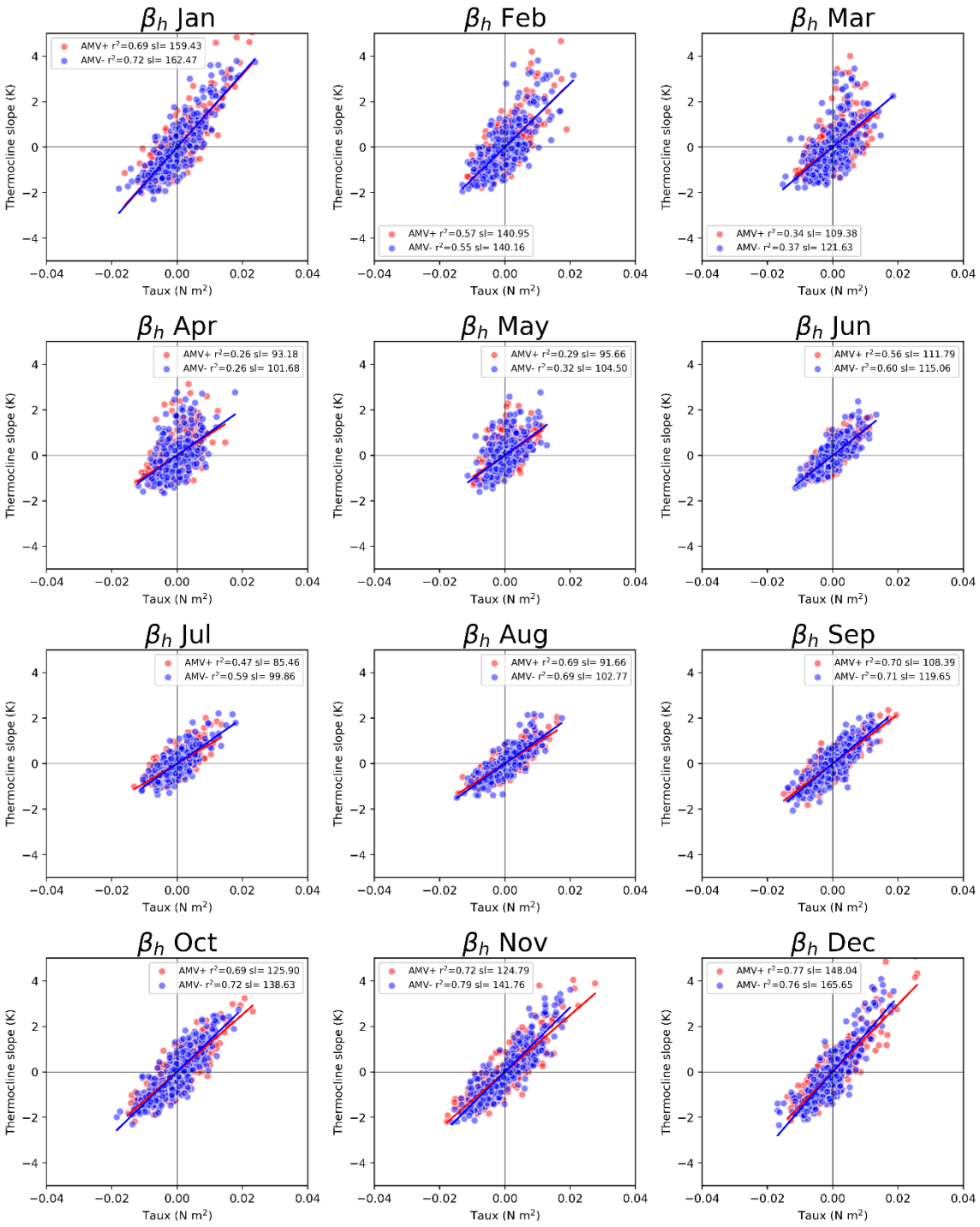

Figure S5. Scatterplot of monthly thermocline slope anomalies vs. equatorial Pacific wind stress anomalies in the AMV+ (red) and AMV- (blue) experiments. The legend shows the regression slope (K^{-1} $(N\ m^2)^{-1}$) and r^2 value.

Methodology to calculate the BJ index

$$2BJ = -\left[a_1 \frac{\langle \Delta\bar{u} \rangle_E}{L_x} + a_2 \frac{\langle \Delta\bar{v} \rangle_E}{L_y}\right]_{CD} - [\alpha_s]_{TD} + \left[\mu_a \beta_u \langle -\frac{\partial \overline{\mathrm{T}}}{\partial \mathrm{x}} \rangle_E\right]_{ZA} + \left[\mu_a \beta_w \langle -\frac{\partial \overline{\mathrm{T}}}{\partial \mathrm{z}} \rangle_E\right]_{EK} + \left[\mu_a \beta_h \langle -\frac{\bar{w}}{H_1} \rangle_E a_h\right]_{TC}$$

The Bjerknes Stability index (hereafter BJ index) is based on the recharge oscillator model (Jin 1997) and was introduced by Jin *et al*. (2006) with the aim of quantifying the different atmosphere and ocean mechanisms involved in ENSO growth rate.

The ENSO growth rate is estimated as the sum of, from left to right, the current damping (CD), thermodynamic (TD), zonal advective (ZA), Ekman (EK) and thermocline (TC) feedbacks. Following previous studies (Jin *et al.* 2006; Guilyardi *et al.* 2009; Kim and Jin 2011a; Kim and Jin 2011b; Kim *et al.* 2014; Lübbecke and Mcphaden 2014; An *et al.* 2017), the BJ index terms are calculated using linear regression between variables across all years in the simulations.

The boundary between the eastern and western Pacific is defined by regressing ocean heat content anomalies onto the timeseries of the first empirical orthogonal function (EOF) of anomalous SSTs. For the CESM1 model, the nodal line crosses the equator at 170°E, hence our eastern Pacific domain extends from 170°E to 80°W and from 5°N to 5°S. The equatorial Pacific domain has the same latitudinal boundaries that the EP region, but reaches 120°E on its western boundary.

1. Current damping

1.1 a_1

Linear regression of the SST difference between the western boundary of the eastern Pacific domain (i.e., averaged SST between 5ºS-5ºN at 170°E) and the eastern boundary of the domain (i.e., averaged SST between 5ºS-5ºN at 80°W) onto the mean SST of the eastern Pacific domain (i.e., averaged SST over 170°E-80°W / 5°N-5°S).

1.2 $\langle \Delta\bar{u} \rangle_E$

Difference of the climatological surface ocean zonal current between the western boundary of the East Pacific domain (5ºS-5ºN at 170°E) and the eastern boundary (5ºS-5ºN at 80°W). Units are m year^{-1}.

1.3 L_x and L_y

L_x is the longitudinal extent of the Eastern Pacific domain, in this case= 14,513,590 m.
L_y is the latitudinal extent = 2,480,797 m.

1.4 a_2

Linear regression of SSTs in the northern boundary of the Eastern Pacific box (5°N) minus SSTs in the southern boundary of the box (5°S) onto mean SSTs in the EP box (170°E-80°W, 5°N-5°S).

First of all, average SSTs between 170°E and 80°W, then extract SST values at the north and south locations and subtract N-S. Use absolute values, not anomalies. Units are K K^{-1}.

1.5 $\langle \Delta \overline{v} \rangle_E$

Climatological surface meridional ocean current difference between the northern boundary of the East Pacific box (5°N) minus southern boundary (5°S). Units are m $year^{-1}$.

2. Thermodynamic

Negative feedback. Longwave, shortwave, latent and sensible heat flux and SST anomalies are averaged over our East Pacific region. Then flux anomalies are regressed onto SST anomalies.

Units are in W m^{-2} K^{-1}, multiply by 0.14 to convert in $years^{-1}$ (Divide by the heat capacity of the water (4180 J kg^{-1} K^{-1}), the density of seawater (1029 kg m^{-3}) and the mixed layer depth (50 m), then multiply by 31,536,000 to convert from $seconds^{-1}$ to $year^{-1}$).

3. Zonal advective

3.1 μ_a

Equatorial Pacific (120°E - 80°W, 5°N - 5°S) wind stress anomalies regressed onto East Pacific (170°E - 80°W, 5°N - 5°S) SST anomalies. Units are 10^{-3} N $m^{-2}K^{-1}$. Area averaged before regression.

3.2 β_u

Regression of EP (170°E - 80°W, 5°N - 5°S) ocean surface zonal current anomalies (10^{-2} m s^{-1}) against equatorial Pacific (120°E - 80°W, 5°N - 5°S) (10-3N m^{-2}). Units are in seconds, multiply by 31,536,000 to get units of $year^{-1}$. Area averaged before regression.

3.3 $\langle -\frac{\partial \overline{T}}{\partial x} \rangle_E$

Mean zonal SST gradient over EP (170°E - 80°W, 5°N - 5°S). Use climatological SSTs, not anomalies.

4. Ekman

See zonal advective feedback for the definition of μ_a

4.1 β_w

Regression of EP (170°E - 80°W) upwelling ocean current anomalies (10^{-2} m s^{-1}): Average values from 0-50m against equatorial Pacific (120°E and 80°W) surface wind stress anomalies (10^{-3}N m^{-2}).

4.2 $\langle -\frac{\partial \overline{T}}{\partial z} \rangle_E$

Mean vertical temperature gradient over EP (average 170°E - 80°W, 5°N - 5°S) from 0 to 50m depth. Use climatological SSTs, not anomalies.

5. Thermocline

See zonal advective feedback for the definition of μ_a

5.1 β_h

Regression of thermocline slope anomalies =difference between EP (170°E - 80°W) and WP (120°E - 170°E) ocean temperatures averaged from the surface to 300m against equatorial Pacific (120°E - 80°W) surface wind stress anomalies.

5.2 $\langle -\frac{\overline{w}}{H_1} \rangle_E$

Climatological upwelling values over the East Pacific (170°E - 80°W) divided by 50 m. Negative w set to 0 instead of masking.

5.3. a_h

Upper ocean heat content (temperatures averaged from 0 to 300m) anomalies in the East Pacific regressed onto temperature anomalies at 50m depth, accounting only for upwelling.

References

An, S.I., Heo, E.S. and Kim, S.T. (2017) 'Feedback process responsible for intermodel diversity of ENSO variability', *Geophysical Research Letters*, 44, 4272-4279.

Guilyardi, E., Braconnot, P., Jin, F.F., Kim, S.T., Kolasinski, M., Li, T. and Musat, I. (2009) 'Atmosphere feedbacks during ENSO in a coupled GCM with a modified atmospheric convection scheme', *Journal of Climate*, 22, 5698-5718.

Jin, F.-F. (1997) 'An Equatorial Ocean Recharge Paradigm for ENSO. Part I: Conceptual Model', *Journal of the Atmospheric Sciences*, 54, 811-829.

Jin, F.F., Kim, S.T. and Bejarano, L. (2006) 'A coupled-stability index for ENSO', *Geophysical Research Letters*, 33.

Kim, S.T., Cai, W., Jin, F.F. and Yu, J.Y. (2014) 'ENSO stability in coupled climate models and its association with mean state', *Climate Dynamics*, 42, 3313-3321.

Kim, S.T. and Jin, F.F. (2011a) 'An ENSO stability analysis. Part I: Results from a hybrid coupled model', *Climate Dynamics*, 36, 1593-1607.

Kim, S.T. and Jin, F.F. (2011b) 'An ENSO stability analysis. Part II: Results from the twentieth and twenty-first century simulations of the CMIP3 models', *Climate Dynamics*, 36, 1609-1627.

Lübbecke, J.F. and Mcphaden, M.J. (2014) 'Assessing the twenty-first-century shift in enso variability in terms of the bjerknes stability index', *Journal of Climate*, 27, 2577-2587.